CO$_2$ utilization in chemical looping gasification and co-gasification of lignocellulosic biomass components over iron-based oxygen carriers
Thermogravimetric behavior, synergistic effect, and reduction characteristics

Kuo, Po Chih; Sun, Zhuang; Özdemir, Faruk; Aziz, Muhammad; Wu, Wei

Important note
To cite this publication, please use the final published version (if applicable).
Please check the document version above.

CO₂ utilization in chemical looping gasification and co-gasification of lignocellulosic biomass components over iron-based oxygen carriers: Thermogravimetric behavior, synergistic effect, and reduction characteristics

Po-Chih Kuo [a],[*],[1], Zhuang Sun [b],[1], Faruk Özdemir [c], Muhammad Aziz [a],[*], Wei Wu [d]

[a] *Institute of Industrial Science, The University of Tokyo, 4-6-1 Komaba, Meguro-ku, Tokyo 153-8505, Japan*
[b] *Department of Mechanical Engineering, The University of Tokyo, 7-3-1 Hongo, Bunkyo-ku, Tokyo 113-8656, Japan*
[c] *Process and Energy Department, Delft University of Technology, Leeghwaterstraat 39, 2628 CB Delft, the Netherlands*
[d] *Department of Chemical Engineering, National Cheng Kung University, Tainan 70101, Taiwan*

ARTICLE INFO

ABSTRACT

Efficient CO₂ utilization in the thermochemical conversion of biomass plays an important role in creating a future low-carbon economy. This study attempts to explore the CO₂-assisted chemical looping gasification and co-gasification process of lignocellulosic biomass components (hemicellulose, cellulose, and lignin) with iron oxide oxygen carriers using thermogravimetry and differential thermal analysis. Three different iron oxide oxygen carrier-to-biomass (O/B) ratios were taken into account to deeply understand the thermal degradation characteristics of individual components (O/B ratio: 0) and their blending with iron oxide oxygen carriers (O/B ratio: 0.5 and 1). Meanwhile, the reduction characteristics of three major biomass components were also investigated in terms of X-ray diffraction (XRD), synergistic interaction, and reduction degree. Experimental results suggest that the existence of iron oxide oxygen carriers could accelerate the reaction kinetics under the reactive CO₂ environment, arising from the competitive relationship between the direct reduction reaction by char in biomass and the Boudouard reaction at high temperatures (600–950 °C). Interestingly, the reoxidation behavior of the reduced iron oxide is observed at high temperatures, especially for lignin. Among all the tested biomass materials, their ability to reduce iron oxide oxygen carriers under the CO₂ atmosphere follows the order of biomass mixture (1:1:1 wt%)>lignin>xylan>cellulose. Moreover, the findings indicate that significant synergistic interaction exists during the CO₂-assisted chemical looping co-gasification process.

1. Introduction

The development of emerging CO₂ conversion and utilization technologies plays an increasingly crucial role in accelerating the energy transition to reach the carbon neutrality goal by 2050. Therefore, to accomplish long-term decarbonization, the efficient reuse of CO₂ has evoked intensive interest in the past few years [1]. Furthermore, in view of the environmentally friendly and carbon-neutral features of biomass resources, negative carbon emissions are potentially achievable by combining bioenergy and CO₂ capture, utilization, and storage (BEC-CUS). At present, a wide variety of BECCUS processes have been evaluated by coupling the thermochemical conversion of biomass and power-to-chemicals technology with biogenic CO₂ recycling [2,3].

To understand the technical feasibility, economics, and sustainability of CO₂ utilization in the thermochemical processes of biomass, numerous works on pyrolysis and gasification under the CO₂ atmosphere have been investigated so far [4,5]. Apart from the conventional gasification process, another prospective approach for biomass thermal conversion is to apply metal oxide oxygen carriers to the gasification process, also known as chemical looping gasification. This technology is able to improve the conversion of biomass and syngas quality due to the synergistic catalytic effect and lattice oxygen accompanied by metal oxide oxygen carriers [6–8]. A review of the literature on the chemical looping gasification of biomass suggests that processes under the

nitrogen atmosphere have been carried out extensively both in a thermogravimetric analyzer (TGA) and a fixed reactor, whereas there have been very rare works that examine the CO_2 environment [9,10]. Bhui and Vairakannu [11] performed the in-situ CO_2 gasification of coal in the presence of iron-based oxygen carriers (Fe_2O_3) in the fixed bed reactor. It was observed that the reactivity of both volatiles-Fe_2O_3 and tar-CO_2 reactions was improved in the CO_2 atmosphere. He et al. [12] conducted chemical looping gasification of biomass over $NiFe_2O_4$ in the TGA to explore the impact of CO_2 on its performance and found that CO_2 as a gasifying agent was able to facilitate the biomass conversion at high temperatures due to the CO_2 gasification of biochar, whereas the inhibition effect on the devolatilization of biomass was observed in the presence of CO_2. Lin et al. [13] tested the chemical looping gasification of pine biomass both in the TGA and fixed reactor. Their experimental results confirmed that char conversion can be promoted in the CO_2 environment, but a higher reaction temperature ($\sim$670 °C) was needed under CO_2 compared to that under Ar ($\sim$540 °C). Wu et al. [6] observed the thermogravimetric characteristics of chemical looping gasification of lignin over bimetallic-based oxygen carriers in the TGA-MS (mass spectrometer). They reported that introducing CO_2 was advantageous in improving the biochar reactivity, thereby generating valuable carbon monoxide. Moreover, the existence of both oxygen carriers ($BaFe_2O_4$) and CO_2 can enhance the reaction kinetics of chemical looping gasification. As a result, these earlier works all confirmed that the CO_2-assisted thermochemical conversion pathway is a promising and effective decarbonization approach for the simultaneous valorization of biomass into valuable biofuels and CO_2 abatement.

As a matter of fact, it has been widely accepted that lignocellulosic biomass is mainly constituted of hemicellulose (20–40%), cellulose (40–50%), and lignin (10–20%) [14]. Consequently, a full understanding of the reaction behaviors and the role played by individual biomass components during the chemical looping gasification is extremely helpful for the selection of biomass feedstocks, optimization of operating conditions, and enhancement of reaction efficiency for practical applications. To this end, as presented in Table 1, a review of past research demonstrates that most of the relevant chemical looping gasification experiments were focused on the thermal degradation behaviors of pure biomass components under the nitrogen or inert atmosphere; nevertheless, relatively very limited information is available on the CO_2 atmosphere. In particular, the synergistic interaction between three major biomass components and metal oxide oxygen carriers during CO_2-assisted chemical looping co-gasification has not yet been explored. In recent years, the use of Fe-based oxygen carriers in chemical looping gasification has attracted significant attention. The main advantages associated with Fe-based oxygen carriers are low cost, wide availability, high reactivity, and environmental benign [15]. Hence, iron oxide is selected as an oxygen carrier in this study.

For the aforementioned reasons, the present work aims to give a deep and comprehensive insight into the characteristics of CO_2-assisted chemical looping gasification of the three major biomass model components (hemicellulose, cellulose, and lignin) with iron oxide (Fe_2O_3) as oxygen carriers. Experiments at various oxygen carrier-to-biomass (O/B) ratios are carried out to analyze and identify the thermal decomposition behaviors of individual constituents and biomass mixture (1:1:1 wt%) via the thermogravimetric analysis-differential thermal analysis (TGA-DTA) technique. More importantly, particular emphasis will also be placed on the synergistic effect of chemical looping co-gasification of the biomass mixture and reduction characteristics of iron oxide oxygen carriers via X-ray diffraction (XRD).

2. Experimental

2.1. Materials

The selected biomass materials in this work were cellulose, hemicellulose, and lignin, which were three primary constituents contained in lignocellulosic biomass. Cellulose (CAS: 9004–34–6) was purchased from Sigma-Aldrich Co., Ltd. Xylan was chosen to represent a hemicellulose model compound. Xylan (CAS: 9014–63–5) and lignin (CAS: 8061–51–6) were both bought from Tokyo Chemical Industry Co., Ltd. Pure iron oxide (Wako Pure Chemical Industries, Ltd., 99.9%) was utilized as an oxygen carrier in the course of the biomass chemical looping process.

2.2. Thermogravimetric analysis (TGA)

TGA was carried out in a TG/DTA analyzer (Rigaku TG-DTA8122) to elucidate the thermal decomposition characteristics of various biomass materials during the chemical looping gasification process. Before carrying out TGA experiments, cellulose, xylan, and lignin, were mechanically mixed thoroughly with iron oxide powders for the three different iron oxide oxygen carrier (OC)-to-biomass mass ratios (O/B ratio, wt/wt), namely, 0, 0.5, and 1.0. The mass weight of each biomass material was fixed at 10 mg for each experiment. After mixing, the prepared biomass-iron oxide mixtures were placed in sealed plastic tubes and stored in a desiccator at room temperature. Then, the mixture was placed on a ceramic crucible, and it was then heated at a linear rate of 20 °C min^{-1} from ambient temperature to 110 °C for a 10 min holding time in order to initially eliminate moisture content in feedstock. Subsequently, the operating temperature of the TG analyzer furnace was further programmed from 110 °C to 1200 °C. The CO_2 flow rate of 100 ml min^{-1} was charged into the TG analyzer furnace. Moreover, TGA experiments of each pure biomass material were also performed in the nitrogen atmosphere for the purpose of comparison. All conducted experiments were repeated at least three times to ensure the reproducibility of the measured data. The reproducibility of the experimental results is presented in the supplementary data (Fig. S1). Detailed experimental conditions for CO_2-assisted chemical looping gasification of biomass are illustrated in Fig. 1.

Table 1
A literature review of chemical looping gasification of the pure biomass components.

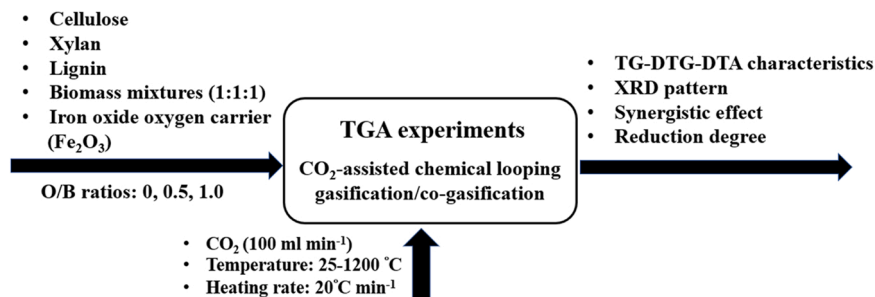| Material	Reactor	Reaction conditions				Literature
		Temperature (°C)	Heating rate (°C min^{-1})	Atmosphere and flowrate (ml min^{-1})	Oxygen carrier	
Cellulose Hemicellulose Lignin	TGA	20–1000	50	N_2 (20)	Fe_2O_3	[29]
Cellulose	Fixed bed	700, 750,800, 850	-	Ar (100)	Fe_2O_3	[35]
Cellulose	TGA Fixed bed	40–1000 (TGA) 800, 850, 900, 950 (Fixed bed)	20 (TGA)	Ar (20) N_2 (20, 40, 60, 80)	CaO, Fe2O3 CaO/Fe2O3 CaFe2O4	[7]
Cellulose	TGA	25–850	10, 20, 40	Ar (60)	Bi2O3 Sb2O3	[24]
Lignin	TGA	25–900	8, 20, 50	N_2 (20)	Fe_2O_3	[33]
Lignin	TGA	10–900	10	He (100) CO_2/He (100)	$BaFe_2O_4$, $BaMn_2O_4$, $CaFe_2O_4$, $CaMn_2O_4$	[6]

Fig. 1. Illustration and operating conditions of experimental analysis in this work.

2.3. X-ray diffraction

XRD (Rigaku MiniFlex 600) measurement was conducted to identify the crystal phase and patterns of the reduced iron oxide oxygen carrier. Monochromatic X-ray was produced by Cu Kα ($\lambda = 0.154$ nm) radiation under an operating voltage of 40 kV and a current of 15 mA. The tested samples were scanned over a range of $2\theta = 30$–$90°$ at a scanning rate of $10°$ min^{-1}. The XRD spectra were subsequently analyzed using the SmartLab Studio II software (Rigaku).

2.4. Synergistic effect of chemical looping co-gasification

The synergistic effects of CO_2-assisted chemical looping co-gasification of biomass mixture (i.e., Cellulose: Xylan: Lignin=1:1:1 wt %) and iron oxide oxygen carriers were experimentally examined. The synergistic effect occurring during the chemical looping co-gasification of biomass blends indicates the promoting or inhibiting effects on reactivity in the co-gasification process. The magnitude of the synergistic parameter (ΔW_{syn}) can be used as an index to explore the synergy behaviors (i.e., promotion/inhibition/none-interaction). The theoretical values were calculated by the linear superposition based on the TG curves of individual biomass components ($W_{theo-mix}$), while the experimental values were obtained from the actual TG curves based on the chemical looping co-gasification of biomass mixture ($W_{exp-mix}$). Therefore, the relative mass loss difference (ΔW_{syn}) affected by the synergistic effect can be expressed as

$$\Delta W_{syn} = W_{\text{exp}-mix} - W_{theo-mix} \tag{1}$$

$$W_{theo-mix} = x_C W_C + x_H W_H + x_L W_L \tag{2}$$

where W_C, W_H, and W_L, are the mass of the cellulose, hemicellulose, and lignin at the three various O/B ratios of 0, 0.5, and 1 (mg), respectively. x_C, x_H, and x_L, are the mass fraction of the cellulose, hemicellulose, and lignin in the blend (%).

Based on the aforementioned equations, the synergistic interaction can be quantitatively examined according to the relative difference in weight loss between the theoretical and experimental values with respect to the investigated temperature range. Physically, the larger the ΔW_{syn}, the greater degree of the synergy of the biomass mixture.

2.5. Reduction degree

To explore the reduction degree of iron oxide reduced by the three biomass materials and biomass mixture, the relative mass loss difference (ΔW_{RD}) between experimental and theoretical values can be quantitatively calculated and defined below:

$$\Delta W_{RD} = W_{theo} - W_{\text{exp}} \tag{3}$$

$$W_{theo} = x_I W_I + x_B W_B \tag{4}$$

where W_{exp} and W_{theo} are the experimental and theoretical values (mg),

respectively. W_I and W_B are the mass of iron oxide and the tested biomass materials (mg), respectively. x_I and x_B are the mass fraction of iron oxide and the tested biomass materials (%).

3. Results and discussion

In the following discussion, the pyrolysis and gasification behaviors, including TG, derivative thermogravimetry (DTG), and differential thermal analysis (DTA), for the three constituents (cellulose, xylan, and lignin) are first discussed. Subsequently, CO_2-assisted chemical looping gasification of the three constituents is examined to realize the effect of iron oxide oxygen carriers on the reactivity performance of biomass. Finally, the synergistic effect between the individual biomass model component or biomass mixture (1:1:1 wt%) and iron oxide oxygen carriers during the CO_2-assisted chemical looping gasification and co-gasification is evaluated.

3.1. Pyrolysis and gasification characteristics

3.1.1. Characteristics of cellulose

The thermal decomposition characteristics of cellulose, xylan, and lignin during pyrolysis and gasification are shown in Figs. 2, 3, and 4, respectively. Based on the distribution of TG and DTG curves, Figs. 2a and 2b display that the thermal decomposition characteristics of cellulose can be roughly classified into four and three reaction zones, corresponding to the CO_2 and N_2 atmospheres, respectively [5,16]. Weight loss of cellulose in the temperature range of 35–125 °C (i.e., 1st reaction zone), which is ascribed to the dehydration of cellulose. Therefore, corresponding to the DTG and DTA curves (Figs. 2b and 2c), a small decomposition peak and an endothermic characteristic appear in both atmospheres. Following the vaporization of moisture, the main thermal degradation of cellulose takes place between 125 and 500 °C (i.e., 2nd reaction zone). In this stage, cellulose is highly reactive due to devolatilization; therefore, an obvious weight loss can be observed, no matter what kind of reaction atmosphere is examined. The weight losses of cellulose under CO_2 and N_2 atmospheres in the second reaction zone are 7.58 and 8.07 mg, respectively, indicating that the reactivity of devolatilization in the CO_2 atmosphere is relatively lower than that in N_2. This could be due to the inhibition effect of CO_2 on the biomass devolatilization process. Similar findings were reported by Dong et al. [4]. They stated that CO_2 may inhibit secondary char formation because of the char-tar interaction in the presence of CO_2. Meanwhile, a great amount of biomass volatiles generated in a short time may inhibit CO_2 diffusion, thus leading to lower weight loss in the CO_2 atmosphere than that in the N_2 one [4]. In addition, He et al. [12] investigated the chemical looping gasification of biomass using $NiFe_2O_4$ as an oxygen carrier under the CO_2 atmosphere via TGA. By comparing the maximum weight loss rates between inert and CO_2 atmospheres, it was also pointed out that using CO_2 as a carrier gas could not improve the reactivity during the devolatilization stage, which can be attributed to the inhibition effect of CO_2 on the biomass volatiles reactions. As seen in the DTG curve (Fig. 2b), the maximum weight loss rate (~ 0.775 mg s^{-1}) is
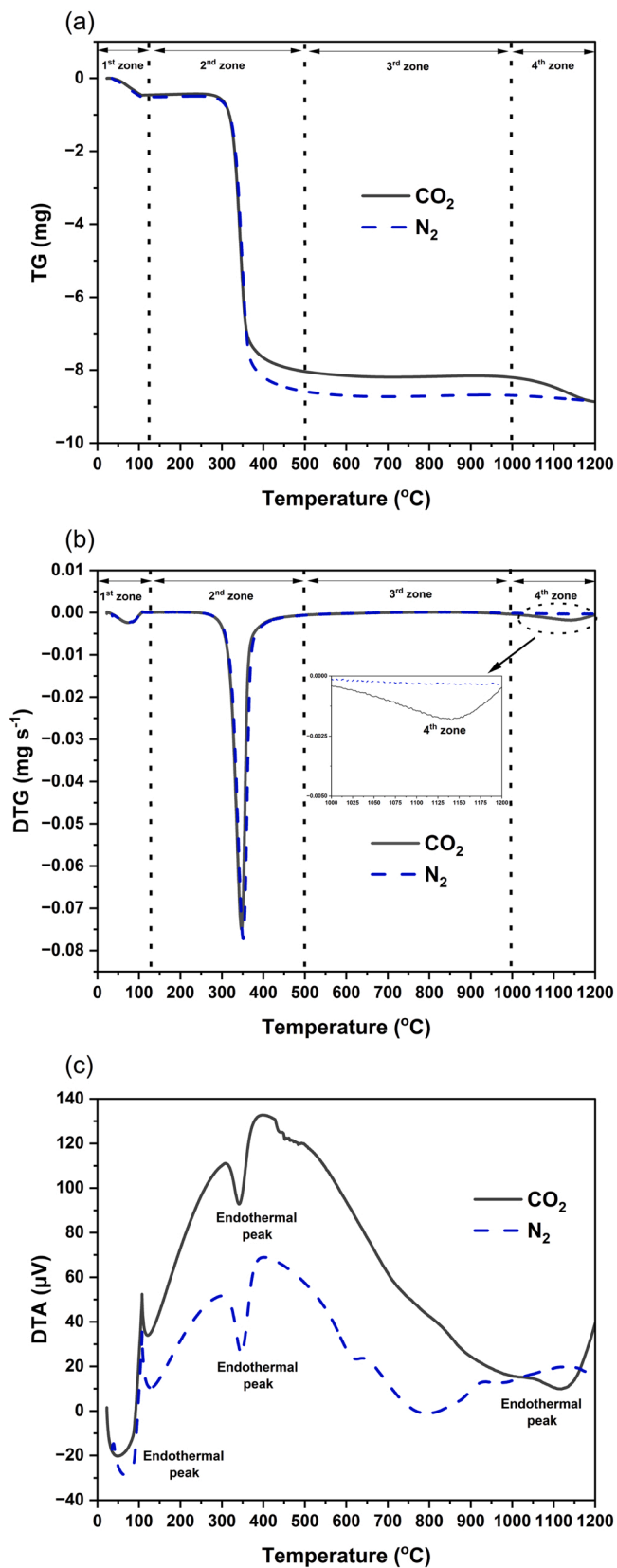
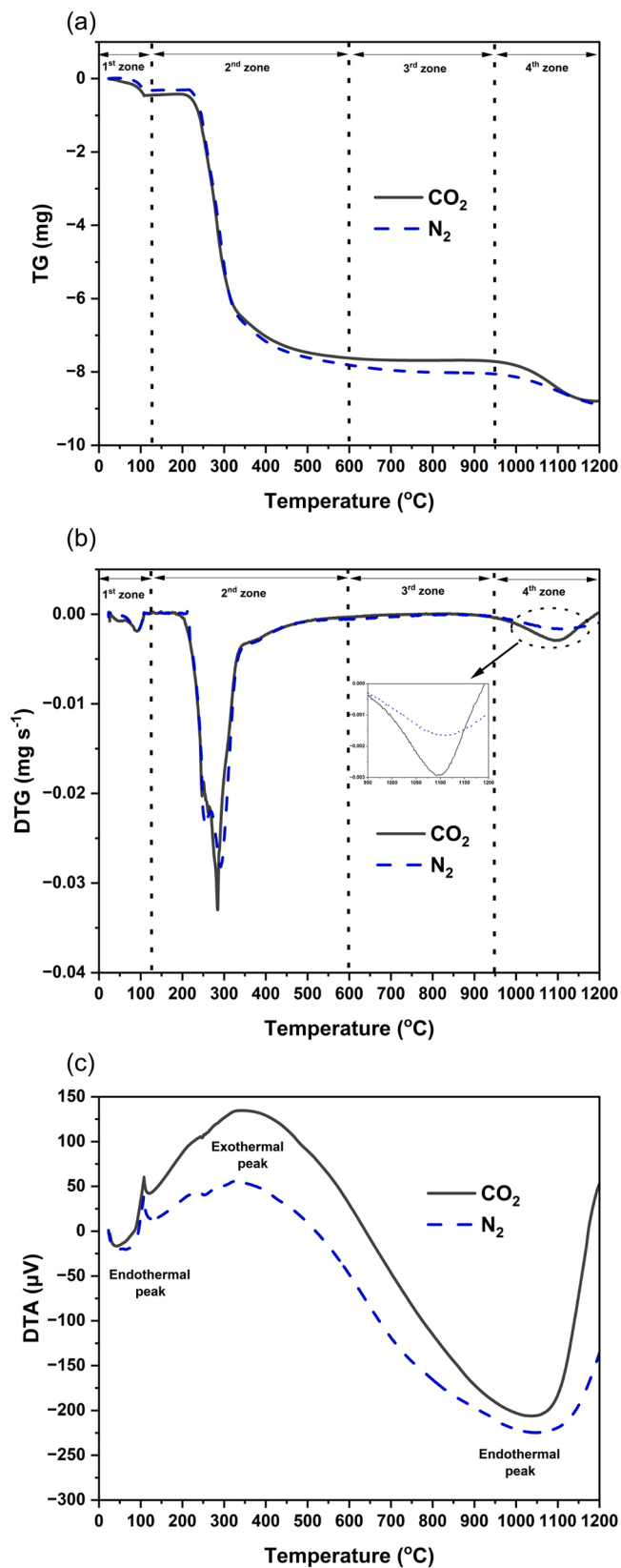**Fig. 2.** Pyrolysis and gasification characteristics of cellulose: (a) TG, (b) DTG, and (c) DTA.

Fig. 3. Pyrolysis and gasification characteristics of xylan: (a) TG, (b) DTG, and (c) DTA.
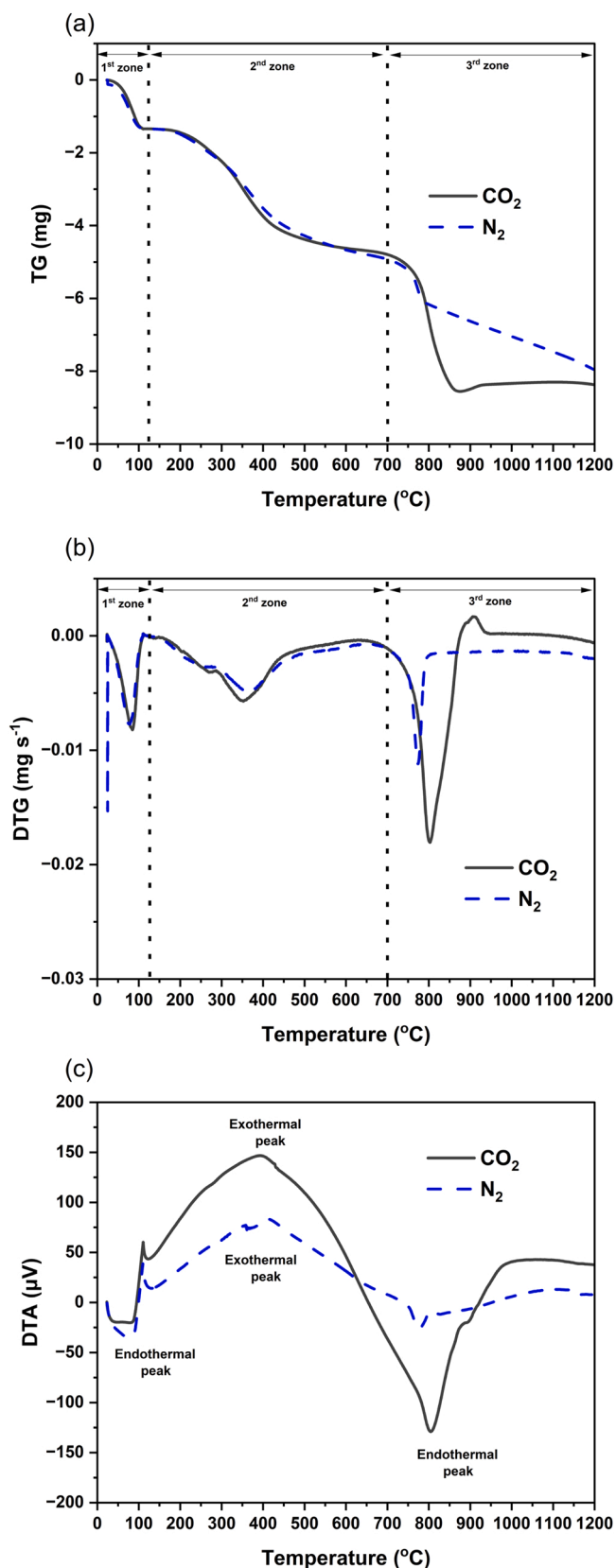
(a)

(b)

(c)

Fig. 4. Pyrolysis and gasification characteristics of lignin: (a) TG, (b) DTG, and (c) DTA.

located at around 350 °C for both atmospheres. Such a DTG peak temperature of cellulose decomposition (300–400 °C) is in accordance with that obtained by Yang et al. [17] and Wang et al. [18]. Meanwhile, it can be seen that the pyrolysis of cellulose exhibits a distinct endothermic feature in both reaction environments. This result is also in agreement with previous studies [17,19]. After the devolatilization region of cellulose, the weight loss (TG) and weight loss rate (DTG) under the N_2 atmosphere do not change significantly when the temperature is higher than 500 °C. This is consistent with the observations in the work of Dong et al. [4]. Again, the reason could be that the inhibition effect of the char-CO_2 reaction would occur as a consequence of the ordered and stable crystalline structures of cellulose [4]. Nevertheless, it is worth noting that the fourth reaction zone between 1000 and 1200 °C can be identified under the CO_2 atmosphere both in the TGA and DTG curves. This could be related to the existence of interaction between biochar and reactive CO_2, stemming from the CO_2 gasification of char, reflecting that a mass loss of around 0.66 mg is examined. Accordingly, an endothermic peak characteristic is indicative of the CO_2 gasification of char (Fig. 2c).

3.1.2. Characteristics of xylan

The distributions of TG, DTG, and, DTA of xylan are shown in Figs. 3a, 3b, and 3c, respectively. Similar to the thermal decomposition behavior of cellulose displayed in Fig. 2, it can be roughly divided into four reaction zones under both N_2 and CO_2 atmospheres according to the TG and DTG curves. Fig. 3a shows that the primary thermal degradation of xylan begins at around 200 °C and decomposes completely at around 600 °C (i.e., 2nd reaction zone). There is no major difference in weight loss between CO_2 (~7.2 mg) and N_2 (~7.5 mg) atmospheres. The DTG curves of the second reaction zone for both atmospheres are also similar, with the maximum weight loss rate (0.027 mg s^{-1}) occurring at around 290 °C. Corresponding to the results from the DTA curve, an obvious exothermic peak characteristic can be identified. Comparable results of the thermal characteristics of xylan were reported by the studies of Zhang et al. [5] and Yang et al. [17]. However, it should be noted that the peak intensity in the DTG curves under the CO_2 atmosphere in the fourth reaction zone is relatively greater than those obtained from the N_2 atmosphere. As expected, this phenomenon can be explained by the increased reactivity of biochar in the presence of a reactive CO_2 environment. The corresponding thermal behavior during the fourth reaction zone is characterized by the endothermic characteristic (Fig. 3c).

3.1.3. Characteristics of lignin

The thermal decompositions characteristics of lignin are plotted in Fig. 4. It is apparent that, unlike cellulose and xylan, the thermal degradation region of lignin occurs over a wide range of temperatures owing to better thermal stability rendered by the aromatic rings [17,19]. Basically, the main decomposition of lignin in CO_2 and N_2 atmospheres mainly consists of two reaction zones at temperatures between 125 and 700 °C (i.e., 2nd reaction zone) and 700–1200 °C (i.e., 3rd reaction zone), as shown in Figs. 4a and 4b. It can be seen that very similar behaviors on the TG and DTG curves in the second reaction zone are observed regardless of reaction atmosphere, whereas those in the third reaction zone remarkably differ from each other. For example, at the second reaction zone, the TG curve under both atmospheres exhibits a two-step of weight change, namely, mass loss of around 0.90 mg between 125 and 300 °C and mass loss of around 2.60 mg between 300 and 700 °C. This behavior, in turn, leads to a double-overlapping peak developed in the DTG curve (Fig. 3b) with the maximum weight loss rate of 0.006 mg s^{-1} in CO_2 (~350 °C) and 0.005 mg s^{-1} (~360 °C) in N_2. Moreover, as shown in Fig. 4c, the thermal behavior in this reaction zone is dominated by exothermic phenomena, which is well in agreement with the findings of Yang et al. [17]. On the contrary, for the third reaction zone, on account of the intensified gasification reaction of char under the CO_2 atmosphere, the magnitude of weight loss in CO_2 is much larger than that in N_2, revealing that the maximum weight loss rate becomes nearly double in the CO_2 environment (Fig. 4b). In comparison

to the exothermic second reaction zone, Fig. 4c indicates that a stronger endothermic peak via the Boudouard reaction appears in the third reaction zone. Notably, the reaction regions of CO_2 gasification of biochar for the three pure biomass materials are consistent with the results observed by Zhang et al. [20].

3.2. Chemical looping gasification characteristics

In this section, the characteristics of CO_2-assisted chemical looping gasification of cellulose, xylan, and lignin are explored. Without adding iron oxide (i.e., O/B=0), CO_2 as a carrier gas for biomass gasification plays an important role at high temperatures (i.e., 3rd and 4th reaction zones) as a result of the dominating char gasification (Figs. 2–4). When blended materials are considered (i.e., O/B=0.5 and O/B=1), the possible reactions typically taking place during the chemical looping gasification process can be classified by the indirect and direct reduction reactions of iron oxide [21]. The former is known as the gas-solid reduction reaction, triggered by biomass volatiles (i.e., H_2, CO, CH_4), which are generated from the pyrolysis and tar cracking processes [22], while the latter is regarded as the solid-solid reduction reaction caused by fixed carbon [23]. Notably, by virtue of using CO_2 as a carrier gas, gasification of biochar also occurs at high temperatures (typically>700 °C). The reaction mechanisms of the reduction process by the three biomass materials are listed in Table 2.

3.2.1. Chemical looping gasification of cellulose

The influence of iron oxide oxygen carriers on the thermal degradation of cellulose under the CO_2 atmosphere is illustrated in Fig. 5. Figs. 5a and 5b. depict that, as expected, iron oxide carriers have an insignificant impact on the behavior of thermal decomposition from room temperature to around 350 °C because the pattern of TG and DTG curves are almost identical. Nevertheless, above 350 °C, the weight loss is increased for both O/B ratios of 0.5 and 1.0, implying that the addition of iron oxide carriers could improve the devolatilization performance of cellulose [7,24]. Specifically, corresponding to the O/B ratios of 0, 0.5, and 1, the maximum weight loss rates of cellulose are 0.075, 0.087, and 0.094 mg s^{-1}, respectively (Fig. 5b). In order to further understand the impact of iron oxide oxygen carriers on the devolatilization stage, a devolatilization index (D_i) is used in this work, which is determined by [25]:

$$D_i = \frac{R_{max}}{T_{in} T_{max} \Delta T_{0.5}}$$

(5)

Table 2
Main chemical reactions occurring during the biomass chemical looping gasification with iron oxide carriers [21–23].

| Reaction mechanisms	Chemical reactions	Heat of reaction (ΔH_{298K}, kJ/mol)
Indirect reduction by CO	R1: $3Fe_2O_3 + CO \rightarrow 2Fe_3O_4 + CO_2$	-43.22
	R2: $Fe_3O_4 + CO \rightarrow 3FeO + CO_2$	19.29
	R3: $FeO + CO \rightarrow Fe + CO_2$	-10.92
	R4: $Fe_2O_3 + 3CO \rightarrow 2Fe + 3CO_2$	-23.39
Indirect reduction by H_2	R5: $3Fe_2O_3 + H_2 \rightarrow 2Fe_3O_4 + H_2O$	-2.07
	R6: $Fe_3O_4 + H_2 \rightarrow 3FeO + H_2O$	60.44
	R7: $FeO + H_2 \rightarrow Fe + H_2O$	30.23
	R8: $Fe_2O_3 + 3H_2 \rightarrow 2Fe + 3H_2O$	100.06
Indirect reduction by CH_4	R9: $FeO + CH_4 \rightarrow Fe + 2H_2 + CO$	236.31
	R10: $Fe_2O_3 + 3CH_4 \rightarrow 2Fe + 6H_2 + 3CO$	718.31
Direct reduction by biochar	R11: $3Fe_2O_3 + C \rightarrow 2Fe_3O_4 + CO$	132.03
	R12: $Fe_3O_4 + C \rightarrow 3FeO + CO$	209.38
	R13: $FeO + C \rightarrow Fe + CO$	155.31
Char gasification (Boudouard reaction)	R14: $C + CO_2 \rightarrow 2CO$	172.47
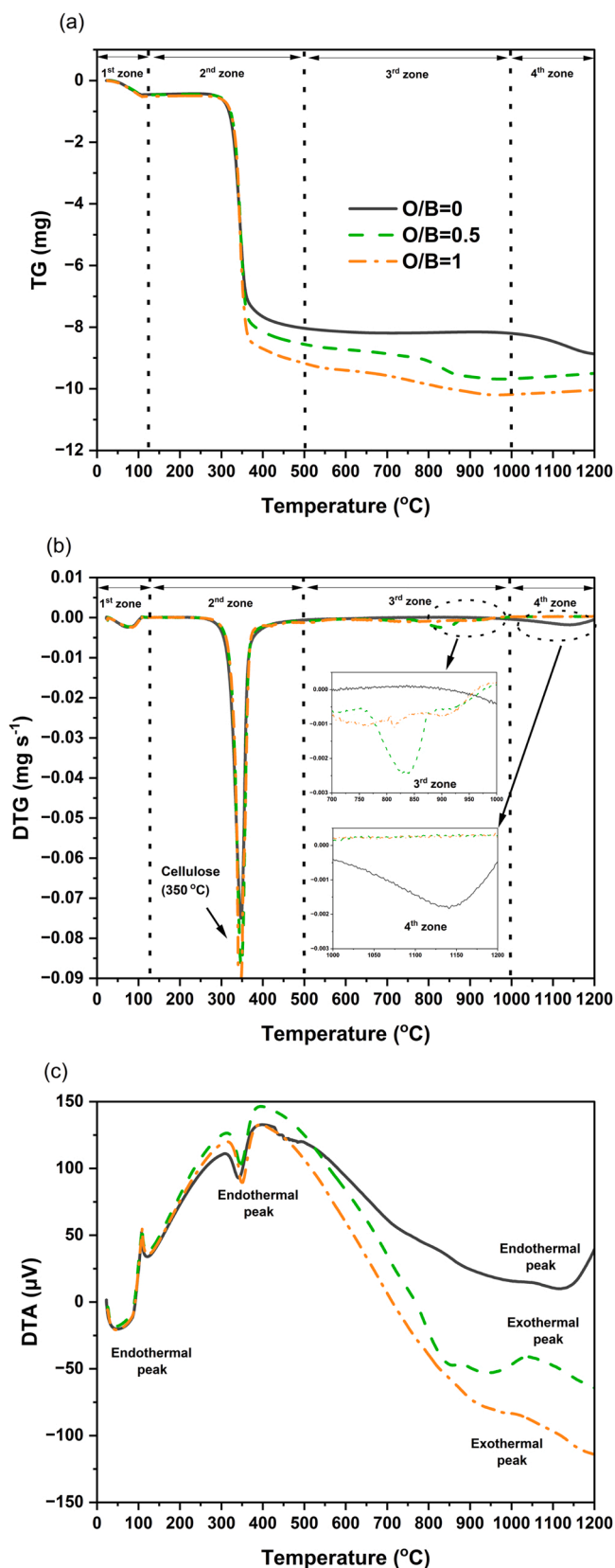
Fig. 5. Chemical looping gasification characteristics of cellulose: (a) TG, (b) DTG, and (c) DTA.

where R_{max} is the maximum weight loss rate during the devolatilization stage. T_{in}, T_{max}, and $\Delta T_{0.5}$ are the initial devolatilization temperature, the temperature of maximum weight loss rate, and the temperature interval when R/R_{max} is equal to 0.5.

The above parameters for calculating D_i can be obtained from the DTG curves, and the higher the value of D_i, the easier the volatiles are released during the devolatilization stage. As presented in Table 3, the values of D_i are increased from 11.1 to 13.3 (10^{-9} mg s^{-1} °C^{-3}) as the O/B ratio increases from 0 to 1. In addition, it is interesting to note that based on the TG curves, the most apparent difference between with and without iron oxide oxygen carriers takes place in the high-temperature range (i.e., 3rd and 4th reaction zones). The above observations can also be confirmed by the distribution of DTG during the same reaction region. In other words, in the third reaction zone, it can be seen that small peaks develop between 700 and 1000 °C in the presence of iron oxide oxygen carriers, whereas those for pure cellulose are not observed. It has been reported that the reaction rate of indirect reduction and char gasification reactions is much faster than the direct reduction reaction [10]. As a result, under the CO_2 atmosphere, the char-CO_2 gasification reaction may be the predominant reaction in this stage, which thereby contributes to the formation of CO utilized for the indirect reduction process [23]. In view of the competing reaction pathways for indirect, direct, and Boudouard reactions (Table 2) in the third stage, no more carbon remains in the fourth reaction zone. Therefore, in contrast to pure cellulose (O/B=0), no peaks are found in this region (O/B=0.5 and O/B=1). This result is consistent with the observation in the DTA curves, where no evident endothermic peak is detected with the addition of iron oxide oxygen carriers, as shown in Fig. 5c. On the other hand, it is very interesting to note that a slight increase in weight is discovered in the fourth reaction zone in the presence of iron oxide oxygen carriers (Fig. 5a). The reason behind this phenomenon could be ascribed to the reoxidation of the reduced iron oxide. A more detailed discussion will be given in Section 3.2.3.

3.2.2. Chemical looping gasification of xylan

Regarding the chemical looping gasification characteristics of xylan, as displayed in Fig. 6, compared with those from cellulose (Fig. 5), it is found that, as shown in Fig. 6a. and 6b, no promoting effect on the primary devolatilization stage (i.e., 2nd reaction zone) is examined with the addition of iron oxide oxygen carriers. For example, as listed in Table 3, the values of D_i are 9.51, 9.20, and 9.56 (10^{-9} mg s^{-1} °C^{-3}), corresponding to the O/B ratio of 0, 0.5, and 1, respectively. On the other hand, similar to cellulose shown in Fig. 5b, the mass loss rate becomes noticeable in the third reaction zone and negligible in the fourth reaction zone with the presence of iron oxide oxygen carriers. Again, it should be pointed out that complex and competing reactions between direct, indirect, and Boudouard reactions simultaneously exist in this stage, resulting in a large portion of biochar being consumed between 600 and 950 °C. Consequently, as shown in Fig. 6c, compared with pure xylan (O/B=0), the exothermic reactions, most likely due to indirect reduction reactions, are observed in these regions, especially for the O/B ratio of 1. Notably, a trend of small weight gain similar to cellulose (Fig. 6a) is found in the fourth reaction zone, most likely due to the reoxidation behavior of the reduced oxygen carriers (see Section 3.2.3).

3.2.3. Chemical looping gasification of lignin

As far as the chemical looping gasification characteristics of lignin are concerned, as plotted in Fig. 7, it can be seen that conversion characteristics of lignin are hardly affected by the addition of iron oxide oxygen carriers over the temperature range of 30–700 °C (Fig.7a) and even somewhat being inhibited, which will be discussed in Section 3.5. As evidenced in Table 3, the values of D_i show a decreasing trend with increasing O/B ratios. In contrast to the devolatilization stage, as shown in Figs. 7a and 7b, it is noteworthy that the presence of iron oxide oxygen carriers could help to facilitate the reaction rate of gasification (i.e., 3rd reaction zone). For instance, the maximum temperature of the DTG peak of pure lignin (O/B=0) in the third reaction zone shifts to a lower temperature from 803 °C to around 780 °C while adding the iron oxide oxygen carriers. This finding is consistent with the study of Wu et al. [6] where various bimetallic oxygen carriers were used for the chemical looping gasification of lignin in the CO_2 atmosphere. They found that the biochar conversion rate is accelerated at higher temperatures in the presence of the oxygen carrier. Regarding the DTA curves of the three O/B ratios (Fig. 7c), it is demonstrated that the endothermic characteristic is exhibited around 800 °C, regardless of what the O/B ratio is.

On the other hand, as mentioned in Sections 3.2.1 and 3.2.2, a weight gain trend can be observed in the fourth reaction zone, regardless of what the biomass material is. Based on the DTG curves in the fourth reaction zone, the weight gain behavior of lignin is much stronger than that of cellulose and xylan. This trend could be explained by the reoxidation behavior of the reduced iron oxide oxygen carriers that took place at higher temperatures [6,12,13]. The phenomenon is more noticeable in the CO_2-assisted chemical looping gasification of the lignin process because lignin has the highest reducibility among the three biomass materials (as verified by XRD analysis in Section 3.5). To further elucidate this phenomenon, a case study of CO_2-assisted chemical looping gasification of lignin was carried out in the temperature range of 25–800 °C. By examining the XRD patterns of the reacted lignin-iron oxide mixture (O/B=1) obtained at 800 °C, as shown in Fig. S2, it can be seen that Fe_2O_3 can be reduced to FeO during the CO_2-assisted chemical looping gasification process. However, when the temperature increases to above 850 °C, FeO is further reoxidized to Fe_3O_4, causing obvious opposite peaks (i.e., positive values of mass loss rate) that occurred at around 850 °C in the DTG curves for the cases of O/B ratios of 0.5 and 1 (Fig. 7b). Similar observations of the reoxidation behavior can be obtained in the works of Wu et al. [6], He et al. [12], and Lin et al. [13]. For instance, Wu et al. [6] showed an increasing trend in weight from 800° to 850°C during the chemical looping gasification of the bimetallic oxygen carrier/lignin mixture and concluded that the reason could be due to the formation of barium carbonate under the CO_2 atmosphere. He et al. [12] investigated the chemical looping gasification of biomass-$NiFe_2O_4$ mixture in the TGA under the CO_2 atmosphere. They pointed out that a weight gain due to the reoxidation of Fe(Ni) reaction occurred at above 850 °C. Similarly, Lin et al. [13] carried out chemical looping gasification of a pine over $NiFe_2O_4$ oxygen carrier in the TGA, and they observed that the reduced oxygen carrier was reoxidized in the CO_2 environment at high temperatures.

However, one should mention that for the case of lignin at O/B= 0, it is surprising that a slight weight gain also appears in the TG curve when the temperate is higher than around 900 °C. It has been well-recognized that internal alkali metal species contained in lignin play an important

Table 3

Characteristic of thermogravimetric analysis of cellulose, xylan, and lignin under various O/B ratios.

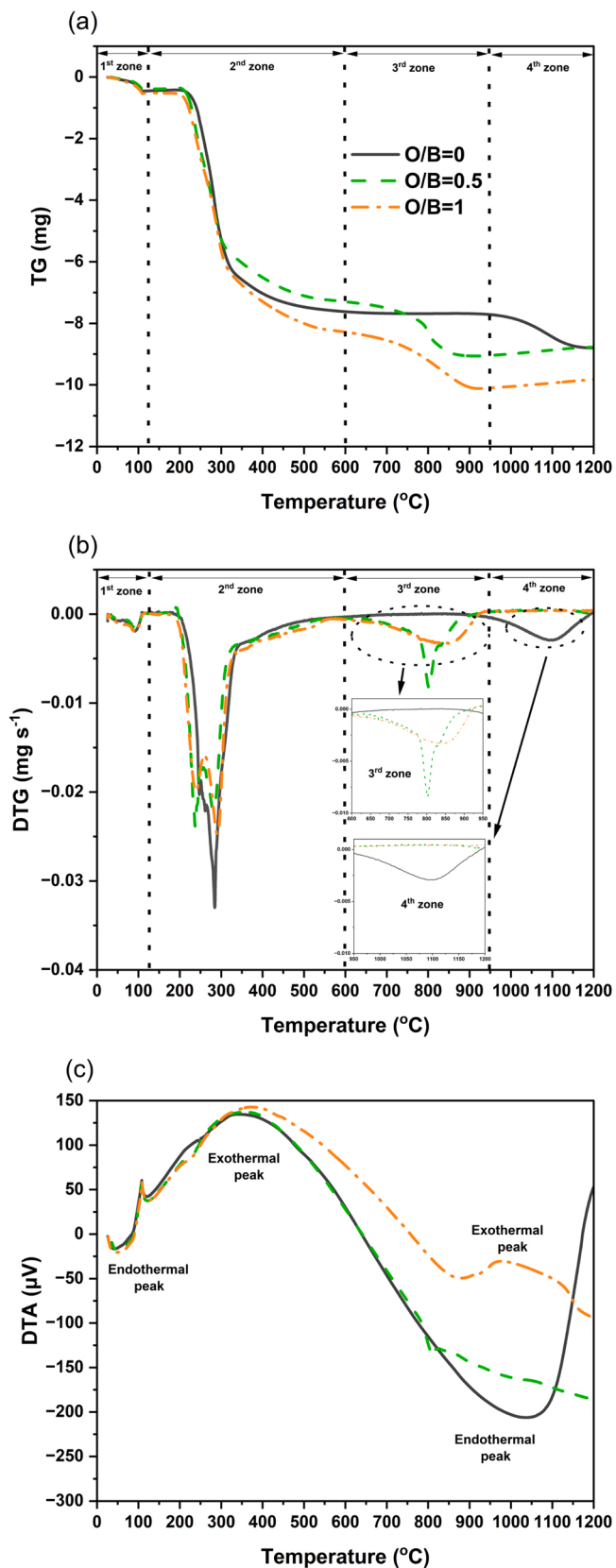|	Cellulose			Xylan			Lignin		
O/B	0	0.5	1	0	0.5	1	0	0.5	1
T_{max} (°C)	347.41	347.64	341.58	284.42	281.69	290.82	352.06	346.24	346.43
$\Delta T_{0.5}$ (°C)	76.36	79.53	81.00	70.10	49.56	53.04	112.73	134.43	139.42
R_{max} (mg s^{-1})	0.075	0.087	0.094	0.033	0.022	0.025	0.006	0.006	0.006
D_i (10^{-9} mg s^{-1} °C^{-3})	11.1	12.4	13.3	9.51	9.20	9.56	0.99	0.85	0.81

Fig. 6. Chemical looping gasification characteristics of xylan: (a) TG, (b) DTG, and (c) DTA.
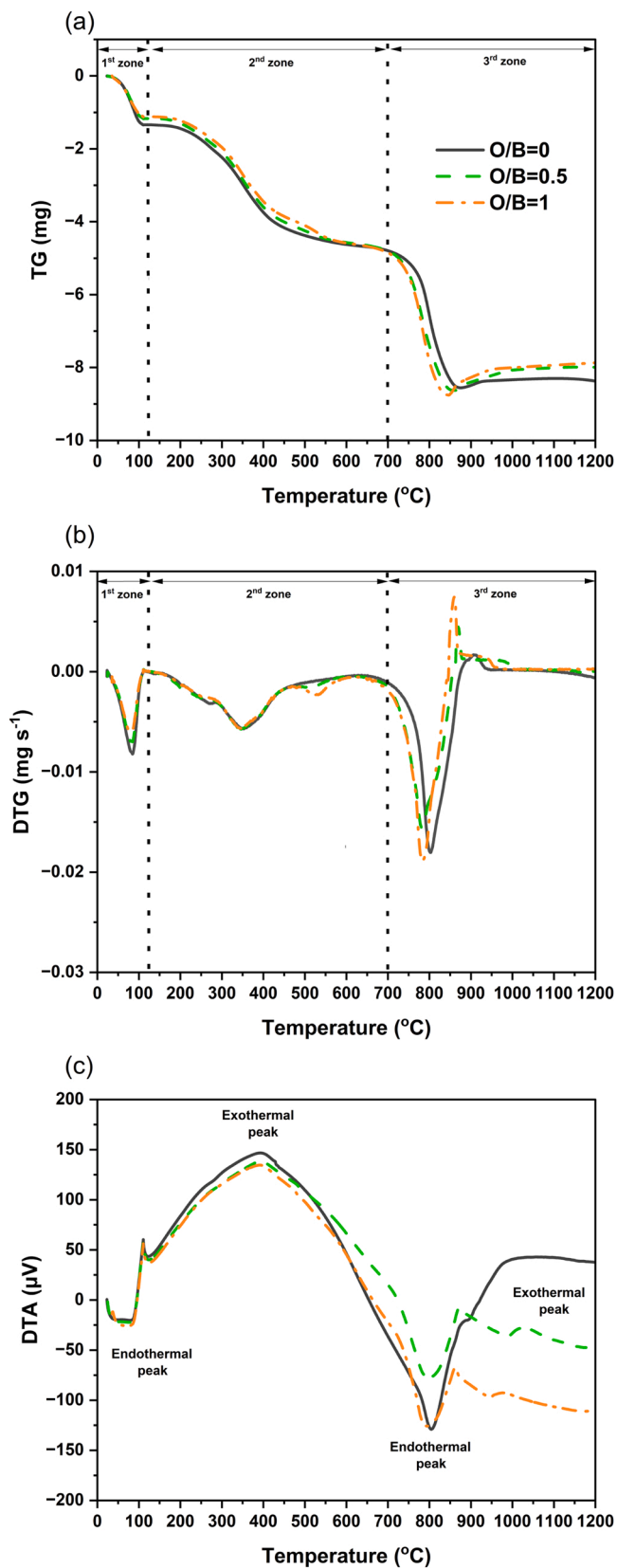

Fig. 7. Chemical looping gasification characteristics of lignin: (a) TG, (b) DTG, and (c) DTA.

role in the performance of pyrolysis and gasification processes [26,27]. The reactivity of CO_2 gasification is essentially affected by the inherent mineral matters in biomass [28]. Therefore, it is probably inferred that the weight gain found at $O/B= 0$ would be related to the interaction between CO_2 and inorganic matter in the char. Further research on the role of minerals in the CO_2 gasification of lignin at the high-temperature reaction zone is required.

3.3. A comparison between CO_2/N_2 atmospheres

For comparison purposes, the thermogravimetric characteristics of the individual biomass components under the N_2 atmosphere are presented in Fig. S3 in the supplementary data, revealing that no obvious differences in the thermal degradation behaviors of the three biomass materials are observed during the devolatilization stage (i.e., 2nd reaction zone), which is also verified by the devolatilization index (Table 1 and Table S1). Nevertheless, a noticeable difference can be found during the iron oxide reduction process (i.e., 3rd reaction zone) due to various reaction mechanisms between the CO_2 and N_2 atmospheres. Under the N_2 atmosphere, the reduction reaction mechanisms are mainly determined by biomass volatiles (mainly H_2 and CO) and biomass-derived biochar [29]. Therefore, both indirect and direct reduction reactions

can possibly contribute to the reduction of iron oxide. By examining the XRD analysis (Fig. S4), it can be seen that Fe_2O_3 is able to be reduced to the FeO phase and Fe phase, except for cellulose under the N_2 atmosphere. The possible phase transformation of iron oxide in the N_2 atmosphere would be Fe_2O_3 (hematite)→Fe_3O_4 (magnetite)→FeO (wustite)→Fe (metallic iron). On the other hand, the endothermic features can be clearly identified in the third reaction zone in N_2, likely due to the direct reduction of iron oxide by biochar (Fig. S3). In contrast, during CO_2-assisted chemical looping gasification of the three biomass materials, the main reaction mechanisms are dominated by indirect reduction and char gasification reactions. Again, the latter ones play a predominant role in yielding a higher amount of CO production due to the presence of reactive CO_2, which further leads to generating more reductant sources for indirect reduction. This, in turn, implies that the direct reduction reaction in the CO_2 atmosphere would be less dominant compared with the N_2 one [10,30]. The reduction characteristics of the iron oxide-biomass mixture in the CO_2 atmosphere would proceed in the following reaction pathway: Fe_2O_3 (hematite)→Fe_3O_4 (magnetite)→ FeO (wustite)→Fe_3O_4 (magnetite). Notably, the reoxidation behavior could take place at higher temperatures (~above 850 °C) in the CO_2-rich environment, as verified in Fig. 10 and Fig. S2.
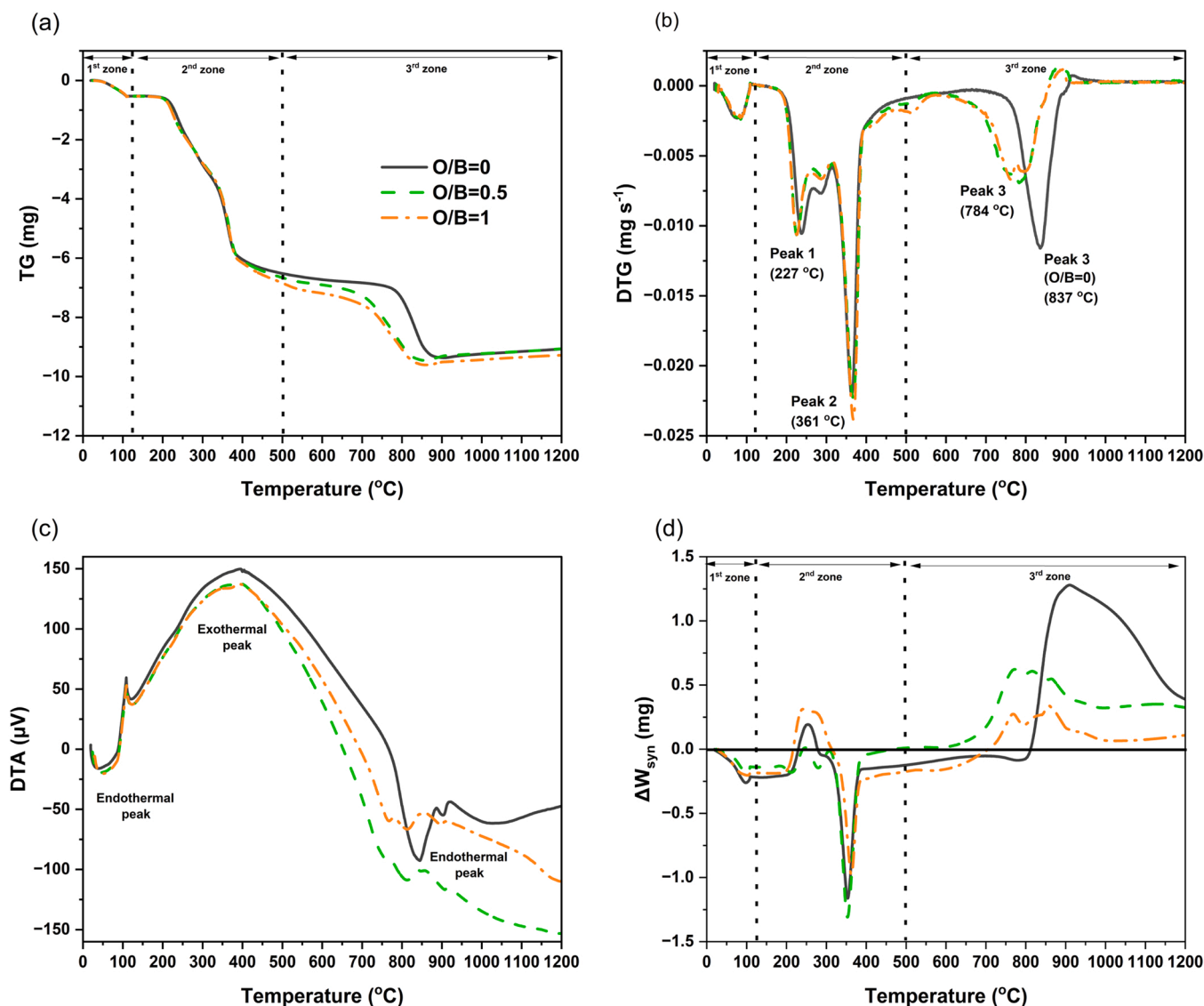

Fig. 8. Chemical looping co-gasification characteristics of biomass mixture: (a) TG, (b) DTG, (c) DTA, and (d) discrepancy value of mass loss (ΔW_{syn}).

3.4. Chemical looping co-gasification and synergistic effect

In order to explore the synergistic effect, the thermal degradation behaviors of CO_2-assisted chemical looping co-gasification of the biomass mixture were conducted. Figs. 8a, 8b, and 8c show the distributions of TG, DTG, and DTA of biomass mixture for various O/B ratios, respectively. It is clear that below 500 °C, a nearly identical trend in the change of mass loss for the three O/B ratios is presented. Basically, three major DTG peaks can be identified between 125 and 1000 °C irrespective of the O/B ratios. Compared with the individual biomass materials (Figs. 5b, 6b, and 7b), it can be seen that the overlapping degradation behaviors between 150 and 500 °C appeared in the second reaction zone, which is mainly attributed to the devolatilization of xylan and cellulose in the same reaction region. The maximum mass loss rate of the first and second DTG peaks for three various O/B ratios are around 0.011 and 0.022 mg s^{-1}, respectively. It is especially noteworthy that, on the one hand, the distributions of DTG with the addition of the iron oxide oxygen carriers are similar to each other, implying that the effect of the O/B ratios on the chemical looping co-gasification of the biomass mixture is not obvious in the second reaction zone. On the other hand, the location of the third DTG peak during the third reaction zone (i.e., peak 3) is completely different between the presence and absence of iron oxide oxygen carriers. For instance, the initial temperature of decomposition for O/B ratios of 0.5 and 1.0 (581 °C) starts lower than that of the pure biomass mixture (675 °C), and their temperature ranges are evident wider. This may be due to the fact that the presence of iron oxide oxygen carriers could substantially promote the reaction rate of biochar under the CO_2 atmosphere [6,12]. In Fig. 8c, the endothermic peak obtained (about 837 °C) from pure biomass mixture is much stronger than the presence of iron oxide oxygen carriers as a result of the dominant char gasification reaction. Fig. 8d shows the degree of the synergistic effects between individual biomass materials and mixture at various O/B ratios, which is evaluated according to Eqs. (1) and (2). The distributions of TG and DTG of iron oxide are shown in the supplementary data (Fig. S5). It is apparent that a significant synergistic interaction exists in the second and third reaction zones, no matter what the O/B ratio is examined. Furthermore, the extent of the synergistic effect for the pure biomass mixture is more remarkable than that of the presence of iron oxide oxygen carriers in a higher temperature zone. The intense synergistic interaction could be attributed to vapor-phase and vapor–solid secondary reactions during the co-gasification of biomass mixture. Such unavoidable secondary reactions include the cracking of heavy hydrocarbons into light ones and volatile-char interactions, which play a significant role in the chemical looping co-gasification of biomass mixture [31,32]. Chen et al. [31] and Yang et al. [32] indicated that the interaction among the three major model components in terms of homogeneous volatile-volatile reaction and heterogeneous char-volatile reaction existed during pyrolysis. In this regard, further investigations into the relationship between volatile and solid reactions from the three biomass model components with iron oxide oxygen carriers in the CO_2 atmosphere are required to be explored in detail.

3.5. Reduction degree

Fig. 9 plots the profile of the reduction degree of iron oxide by each biomass material and their mixtures at an O/B ratio of 1, according to Eqs. (3) and (4). Overall, the discrepancy value of mass loss for cellulose (i.e., 300–400 °C and 800–1050 °C) and xylan (i.e., 200–300 °C and 700–1050 °C) demonstrated a two-stage pattern, while that of lignin is only observed in one stage (i.e., 650–950 °C). For the case of biomass mixture, it can be seen that each peak location is almost the same as that obtained from the individual biomass components. Notably, in the temperature range of 125–500 °C, cellulose has the greatest discrepancy value of the mass loss, whereas lignin has the lowest one among the three biomass model materials. This implies that iron oxide oxygen carriers could potentially have the strongest impact on cellulose,
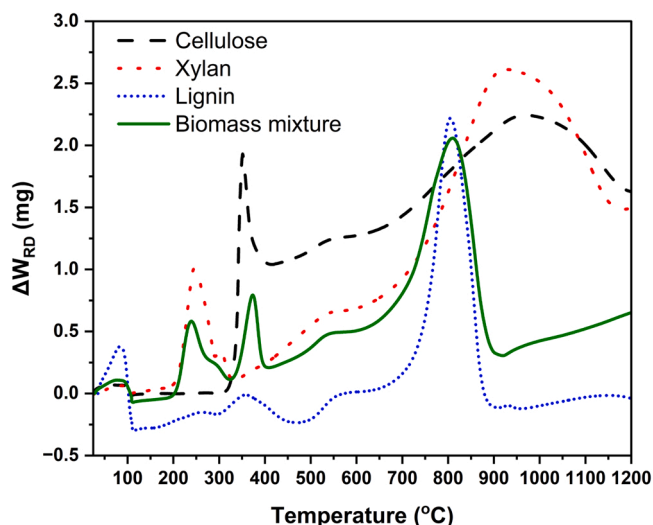

Fig. 9. Reduction degree during CO_2-assisted chemical looping gasification and co-gasification.

whereas the least one on lignin among the three tested materials during the devolatilization stage. Nevertheless, one should mention that lignin even exhibits the negative discrepancy value of mass loss. This phenomenon could be reflected by examining the behavior of chemical looping gasification of lignin. Comparing the TG profiles in the second reaction zone (Fig. 7a), it is found that the weight loss at an O/B ratio of 0 was slightly lower than that at the O/B ratios of 0.5 and 1. The reason for this would be attributed to poor gas diffusion of CO_2 to the lignin surface, thereby hindering the effective contact of the gas-solid reaction [33]. This, in turn, leads to obtaining negative values of reduction degree at a lower temperature range. In addition, Wei et al. [33] also indicated that the poor contact between lignin and iron oxide would be caused by the foaming of lignin during the heating process.

The aforementioned results are consistent with those obtained from the distributions of DTG of individual biomass components (Figs. 5b, 6b, and 7b). Conversely, it is worth noting that for the cases of cellulose and xylan, the peaks developed at high temperatures disappear when three biomass materials are blended, reflecting that the reaction mechanisms are remarkably altered. This may be explained by the significant synergistic interaction between biomass volatiles during the secondary reactions and iron oxide oxygen carriers [32,34]. Hence, the behaviors of CO_2-assisted chemical looping co-gasification of biomass could not be simply predicted according to the additive rule because of the synergistic interaction.

Fig. 10 plots the XRD patterns of each reduced sample at the O/B ratio of 1. As a whole, the crystal phase for magnetite (Fe_3O_4) is detected after CO_2-assisted chemical looping gasification, reflecting that hematite (Fe_2O_3) can be reduced by biomass volatiles or biochar, irrespective of biomass model type. It should be noted that hematite (main peaks occur at 2θ=24.3, and 33.1) still can be identified for the cases of cellulose and xylan, whereas only magnetite (main peaks occur at 2θ=29.9, 35.6, 42.9, 57.1, and 62.7) is observed for lignin, reflecting that the reduction intensity of the former materials is relatively weaker than that of the latter. Interestingly, the strongest intensity of magnetite is identified for the case of biomass mixture. This also clearly suggests that a certain extent of interaction among hemicellulose, cellulose, and lignin existed in CO_2-assisted chemical looping co-gasification. In summary, among all the tested biomass materials, their ability to reduce iron oxide oxygen carriers under the CO_2 atmosphere is followed in descending order by biomass mixture, lignin, xylan, and cellulose.
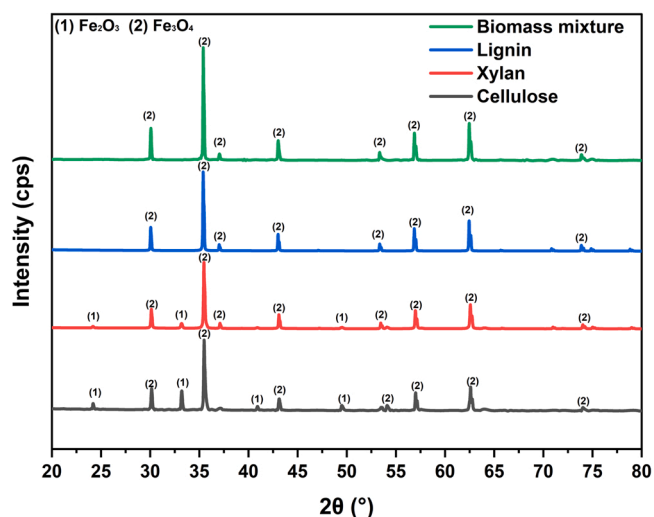
Fig. 10. XRD pattern of iron oxide oxygen carriers.

4. Conclusions

In this work, the CO_2-assisted chemical looping co-gasification of the three biomass model components (i.e., cellulose, hemicellulose, and lignin) and their blends (1:1:1 wt%) was investigated using TGA. The obtained results showed that for a lower temperature range, iron oxide oxygen carriers had a positive impact on the thermal decomposition of cellulose, whereas a slight inhibition effect for lignin was observed. However, for a higher temperature range, iron oxide oxygen carriers play an important role in the acceleration of reaction kinetics under the reactive CO_2 environment due to the competitive interaction between the direct reduction and Boudouard reactions. A comparison between theoretical and actual values of mass loss indicated that significant synergistic interaction was found during CO_2-assisted chemical looping co-gasification of biomass mixture. In addition, an examination of reduction characteristics revealed that the synergistic effect was also observed between biomass mixture and iron oxide oxygen carriers, especially for the cases of cellulose and xylan. According to the XRD analysis of the tested biomass materials, it was found that the reduction ability of each biomass material was ranked in descending order as follows: biomass mixture (1:1:1 wt%)>lignin>xylan>cellulose. Further investigations will be considered in reaction kinetic mechanisms and the product characteristics (i.e., gas, liquid, solid, and conversion efficiency) based on laboratory-scale fixed bed reactor in our future work.

CRediT authorship contribution statement

Po-Chih Kuo: Conceptualization, Writing – review & editing, Investigation, Funding acquisition. **Zhuang Sun:** Conceptualization, Investigation, Writing – review & editing. **Faruk Özdemir:** Writing – review & editing. **Muhammad Aziz:** Conceptualization, Resources, Writing – review & editing, Funding acquisition. **Wei Wu:** Writing – review & editing.

Declaration of Competing Interest

The authors declare that they have no known competing financial interests or personal relationships that could have appeared to influence the work reported in this paper.

Data Availability

Data will be made available on request.

Appendix A. Supporting information

Supplementary data associated with this article can be found in the online version at doi:10.1016/j.jece.2023.109971.

References

[1] S. Saeidi, N.A.S. Amin, M.R. Rahimpour, Hydrogenation of CO_2 to value-added products-a review and potential future developments, J. CO_2 Util. 5 (2014) 66–81.

[2] C. Panzone, R. Philippe, A. Chappaz, P. Fongarland, A. Bengaouer, Power-to-Liquid catalytic CO_2 valorization into fuels and chemicals: focus on the Fischer-Tropsch route, J. CO_2 Util. 38 (2020) 314–347.

[3] B.C. Jaspers, P.C. Kuo, A. Amladi, W. Van Neerbos, P.V. Aravind, Negative CO_2 emissions for transportation, Front. Energy Res. 9 (2021), 626538.

[4] Z. Dong, Z. Liu, X. Zhang, H. Yang, J. Li, S. Xia, Y. Chen, H. Chen, Pyrolytic characteristics of hemicellulose, cellulose and lignin under CO_2 atmosphere, Fuel 256 (2019), 115890.

[5] J. Zhang, T. Chen, J. Wu, J. Wu, Multi-Gaussian-DAEM-reaction model for thermal decompositions of cellulose, hemicellulose and lignin: Comparison of N_2 and CO_2 atmosphere, Bioresour. Technol. 166 (2014) 87–95.

[6] J. Wu, L. Bai, H. Tian, J. Riley, R. Siriwardane, Z. Wang, T. He, J. Li, J. Zhang, J. Wu, Chemical looping gasification of lignin with bimetallic oxygen carriers, Int. J. Greenh. Gas Control 93 (2020), 102897.

[7] G. Tang, J. Gu, Z. Huang, H. Yuan, Y. Chen, Cellulose gasification with Ca-Fe oxygen carrier in chemical-looping process, Energy 239 (2022), 122204.

[8] W. Wu, F. Wen, J. Chen, P. Kuo, B. Shi, Comparisons of a class of IGCC polygeneration/power plants using calcium/chemical looping combinations, J. Taiwan Inst. Chem. Eng. 96 (2019) 193–204.

[9] J. Zeng, R. Xiao, S. Zhang, H. Zhang, D. Zeng, Y. Qiu, Z. Ma, Identifying iron-based oxygen carrier reduction during biomass chemical looping gasification on a thermogravimetric fixed-bed reactor, Appl. Energy 229 (2018) 404–412.

[10] Q. Hu, D. Yao, Y. Xie, Y. Zhu, H. Yang, Y. Chen, H. Chen, Study on intrinsic reaction behavior and kinetics during reduction of iron ore pellets by utilization of biochar, Energy Convers. Manag. 158 (2018) 1–8.

[11] B. Bhui, P. Vairakannu, Experimental and kinetic studies on in-situ CO_2 gasification based chemical looping combustion of low ash coal using Fe_2O_3 as the oxygen carrier, J. CO_2 Util. 29 (2019) 103–116.

[12] F. He, Z. Huang, G. Wei, K. Zhao, G. Wang, X. Kong, Y. Feng, H. Tan, S. Hou, Y. Lv, G. Jiang, Y. Guo, Biomass chemical-looping gasification coupled with water/CO_2-splitting using $NiFe_2O_4$ as an oxygen carrier, Energy Convers. Manag. 201 (2019), 112157.

[13] Y. Lin, H. Wang, Z. Huang, M. Liu, G. Wei, Z. Zhao, H. Li, Y. Fang, Chemical looping gasification coupled with steam reforming of biomass using $NiFe_2O_4$: kinetic analysis of DAEM-TI, thermodynamic simulation of OC redox, and a loop test, Chem. Eng. J. 395 (2020), 125046.

[14] P. McKendry, Energy production from biomass (part 1): overview of biomass, Bioresour. Technol. 83 (2002) 37–46.

[15] Z. Huang, G. Xu, Z. Deng, K. Zhao, F. He, D. Chen, G. Wei, A. Zheng, Z. Zhao, H. Li, Investigation on gasification performance of sewage sludge using chemical looping gasification with iron ore oxygen carrier, Int J. Hydrog. Energy 42 (2017) 25474–25491.

[16] Z. Ma, J. Wang, Y. Yang, Y. Zhang, C. Zhao, Y. Yu, S. Wang, Comparison of the thermal degradation behaviors and kinetics of palm oil waste under nitrogen and air atmosphere in TGA-FTIR with a complementary use of model-free and model-fitting approaches, J. Anal. Appl. Pyrolysis 134 (2018) 12–24.

[17] H. Yang, R. Yan, H. Chen, D.H. Lee, C. Zheng, Characteristics of hemicellulose, cellulose and lignin pyrolysis, Fuel 86 (2007) 1781–1788.

[18] J. Wang, B. Shen, D. Kang, P. Yuan, C. Wu, Investigate the interactions between biomass components during pyrolysis using in-situ DRIFTS and TGA, Chem. Eng. Sci. 195 (2019) 767–776.

[19] W.H. Chen, P.C. Kuo, Torrefaction and co-torrefaction characterization of hemicellulose, cellulose and lignin as well as torrefaction of some basic constituents in biomass, Energy 36 (2011) 803–811.

[20] S. Zhang, S. Yu, Q. Li, B.A. Mohamed, Y. Zhang, H. Zhou, Insight into the relationship between CO_2 gasification characteristics and char structure of biomass, Biomass Bioenerg. 163 (2022) 106537.

[21] G. Sun, B. Li, H. Guo, W. Yang, S. Li, J. Guo, Thermodynamic study on reduction of iron oxides by $H_2+CO+CH_4+N_2$ mixture at 900 °C, Energies 13 (2020) 5053.

[22] M.C. Bagatini, T. Kan, T.J. Evans, V. Strezov, Iron ore reduction by biomass volatiles, J. Sustain. Met. 7 (2021) 215–226.

[23] U. Kumar, S. Maroufi, R. Rajarao, M. Mayyas, I. Mansuri, R.K. Joshi, V. Sahajwalla, Cleaner production of iron by using waste macadamia biomass as a carbon resource, J. Clean. Prod. 158 (2017) 218–224.

[24] S. Pinzia, C. Buratti, P. Bartocci, G. Marseglia, F. Fantozzi, M. Barbanera, A simplified method for kinetic modeling of coffee silver skin pyrolysis by coupling pseudo-components peaks deconvolution analysis and model free-isoconversional methods, Fuel 278 (2020), 118260.

[25] W. Guo, R. Zhang, J. Shang, H. Zhang, B. Yang, Z. Wu, Thermal behavior and kinetics analysis from liquid chemical looping gasification of cellulose with bismuth-based and antimony-based oxygen carriers, Fuel 321 (2022), 124047.

[26] S. Wang, Z. Li, X. Bai, W. Yi, P. Fu, Influence of inherent hierarchical porous char with alkali and alkaline earth metallic species on lignin pyrolysis, Bioresour. Technol. 268 (2018) 323–331.

[27] J. Yu, Q. Guo, Y. Gong, L. Ding, J. Wang, G. Yu, A review of the effects of alkali and alkaline earth metal species on biomass gasification, Fuel Process. Technol. 214 (2021), 106723.

[28] R. Roncancio, J.P. Gore, CO$_2$ char gasification: a systematic review from 2014 to 2020, Energy Convers. Manag X 10 (2021), 100060.

[29] R. Wei, D. Xiang, H. Long, C. Xu, J. Li, Reduction of iron oxide by lignin: characteristics, kinetics and Superiority, Energy 197 (2020), 117203.

[30] K.-I. Otsuka, D. Kunii, Reduction of powdery ferric oxide mixed with graphite particles, J. Chem. Eng. Jpn 2 (1969) 46–50.

[31] Y. Chen, Y. Fang, H. Yang, S. Xin, X. Zhang, X. Wang, H. Chen, Effect of volatiles interaction during pyrolysis of cellulose, hemicellulose, and lignin at different temperatures, Fuel 248 (2019) 1–7.

[32] H. Yang, M. Liu, Y. Chen, S. Xin, X. Zhang, X. Wang, H. Chen, Vapor–solid interaction among cellulose, hemicellulose and lignin, Fuel 263 (2020), 116681.

[33] R. Wei, H. Li, Y. Lin, L. Yang, H. Long, C. Xu, J. Li, Reduction characteristics of iron oxide by the hemicellulose, cellulose, and lignin components of biomass, Energy Fuels 34 (2020) 8332–8339.

[34] L. Yi, N. Zhang, H. Hao, L. Wang, H. Xiao, G. Li, Z. Liang, Z. Huang, T. Jiang, Synergetic conversion laws of biomass and iron ore for syngas and direct reduced iron co-production, J. Clean. Prod. 363 (2022), 132387.

[35] Z. Wu, B. Zhang, S. Wu, G. Li, S. Zhao, Y. Li, B. Yang, Chemical looping gasification of lignocellulosic biomass with iron-based oxygen carrier: products distribution and kinetic analysis on gaseous products from cellulose, Fuel Process. Technol. 193 (2019) 361–371.